The 5th Joint International Conference on Multibody System Dynamics
June 24 – 28, 2018, Lisboa, Portugal

Limitations of finite difference methods in the computation of coupling forces prescribed by the Reynolds equation

Luboš Smolík[1], Jan Rendl[1], Martin Hartl[2] and Pavel Polach[1]

[1]*New Technologies for the Information Society, University of West Bohemia, {carlist,rendlj,ppolach}@ntis.zcu.cz*
[2]*Institute of Machine and Industrial Design, Brno University of Technology, hartl@fme.vutbr.cz*

ABSTRACT — *This paper deals with the numerical modelling of journal bearings. They are mainly used for supporting rotating systems and powertrains. The bearing joint can be mathematically represented by a non-linear hydrodynamic force or linearised coefficients of stiffness and damping. The pressure distribution in a thin viscous oil film is described by the Reynolds equation, which can be solved in a basic form only by numerical methods. This paper aims at solving and applying the finite difference method. Moreover, problems and characteristic properties of the chosen method are described in detail.*

1 Introduction

Thin viscous fluid films, which carry load due to the effect of aero- or hydrodynamic lubrication, represent an important family of non-linear couplings in multi-body systems. These films can be found in radial and thrust hydrodynamic bearings, between pistons and liners, in linear and radial aerodynamic bearings and in lubricated contacts. Thus, the accurate evaluation of forces that arise in the viscous films is essential for the computation of dynamics of multi-body systems including powertrains and rotating systems.

The forces in the viscous films can be evaluated as an integral of the pressure distribution of the film over a lubricated surface. The distribution is governed by the Reynolds equation, a partial differential equation, which can be derived from the Navier-Stokes equations [1]. The Reynolds equation can be solved analytically only in special cases [2] and generally has to be solved numerically. Currently, finite element (FEM) [3, 4], finite volumes (FVM) [5] and finite difference (FDM) [1] methods are the most prominent numerical methods for solving this equation.

In order to reduce CPU times, the aero- and hydrodynamic forces are often represented by direct and cross-coupled stiffness and damping coefficients, which can be linear [6] or non-linear [7]. The linear coefficients are common especially in industrial practice – for example almost all manufacturers of journal bearings provide data-sheets with not only design parameters but also with the stiffness and the damping coefficients at several speeds. A customer is then able to perform a dynamic analysis of a rotor supported in the proposed bearings. Some recent articles [8, 9] suggest that numerically obtained functions which describe dependence of the coefficients on journal's speed may not be continuous, although the same functions obtained analytically are continuous and smooth [2].

Discontinuities of the above-mentioned numerically obtained functions are studied in this article in the case of a generic journal bearing, its root cause is identified and possible ways of mitigating its impact on results are discussed. The paper is outlined as follows: the Reynolds equation, evaluation of the hydrodynamic forces and dynamic coefficients are introduced in Section 2, numerical analysis of the above-mentioned discontinuities is discussed in Section 3, and finally Section 4 draws some conclusions and recommendations.

2 Evaluation of hydrodynamic forces

A generic journal bearing shown in Fig. 1a, which consists of a rigid journal and a rigid shell separated with a thin viscous film, is studied in this paper. Distribution of hydrodynamic pressure $p = p(s, x, t)$ in the film is governed

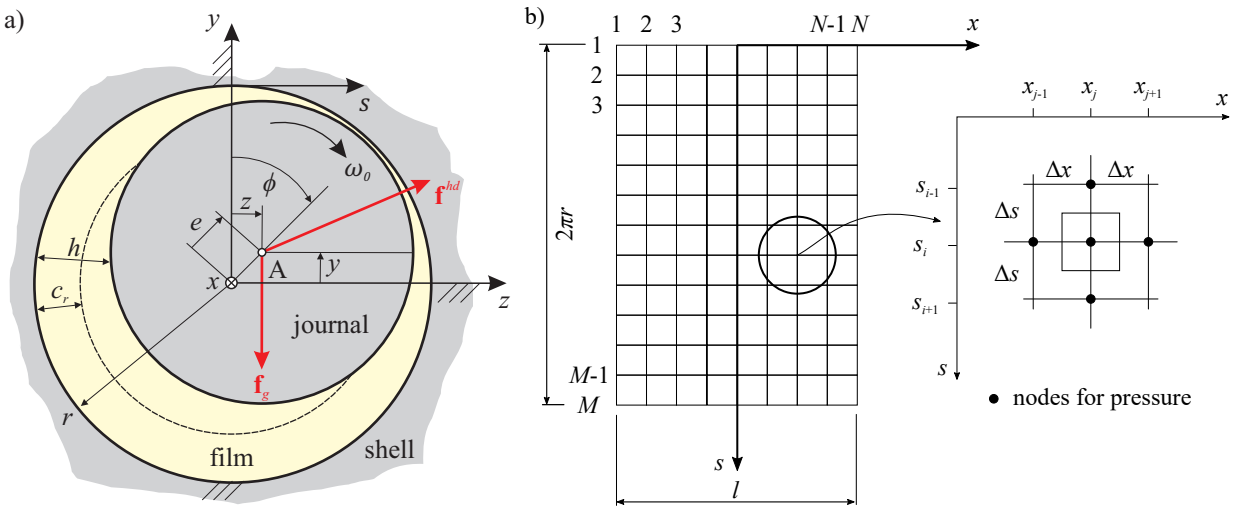

Fig. 1: a) A scheme of a generic journal bearing and b) a mesh for the finite difference method

by the Reynolds equation in the form [1]

$$\frac{\partial}{\partial s}\left(\frac{h^3}{\mu}\frac{\partial p}{\partial s}\right)+\frac{\partial}{\partial x}\left(\frac{h^3}{\mu}\frac{\partial p}{\partial x}\right)=6\,\omega_0\,r\,\frac{\partial h}{\partial s}+12\,\frac{\partial h}{\partial t}, \tag{1}$$

where s and x are the circumferential and axial coordinates, respectively, $h=h(s,\,t)$ is a gap between the journal and the shell, μ is the dynamic viscosity of the film, r is the radius of the bearing and ω_0 is the constant angular speed of the journal. In the case that both the journal and the shell are circular, h is given as

$$h=c_r-e\cos\left(\frac{s}{r}-\phi\right), \tag{2}$$

where c_r is the radial clearance and $e=e(t)$, $\phi=\phi(t)$ are the eccentricity and the angle to eccentricity, respectively. Both e and ϕ are depicted in Fig. 1a.

In order to be solvable by means of the FDM, Eq. (1) has to be reformulated. Firstly, the product rule has to be applied to partial derivatives on its left side. Equation (1) then comes into the form

$$3\frac{h^2}{\mu}\frac{\partial h}{\partial s}\frac{\partial p}{\partial s}+\frac{h^3}{\mu}\frac{\partial^2 p}{\partial s^2}+3\frac{h^2}{\mu}\frac{\partial h}{\partial x}\frac{\partial p}{\partial x}+\frac{h^3}{\mu}\frac{\partial^2 p}{\partial x^2}=6\,\dot{\phi}\,r\,\frac{\partial h}{\partial s}+12\,\frac{\partial h}{\partial t}. \tag{3}$$

Next, the bearing shell has to be covered by a mesh. Usually, a structured regular mesh with Δx step in axial and Δs step in circumferential direction, which is shown in Fig. 1b, is used. The partial derivatives of hydrodynamic pressure p in Eq. (3) can be replaced by finite differences employing the central difference formula, whereas partial derivatives of bearing gap h can be computed analytically. The partial derivatives of p are of the form

$$\frac{\partial p_{i,j}}{\partial s} = \frac{p_{i+1,j}-p_{i-1,j}}{2\Delta s}, \tag{4}$$

$$\frac{\partial^2 p_{i,j}}{\partial s^2} = \frac{p_{i+1,j}-2p_{i,j}+p_{i-1,j}}{\Delta s^2}, \tag{5}$$

$$\frac{\partial p_{i,j}}{\partial x} = \frac{p_{i,j+1}-p_{i,j-1}}{2\Delta x}, \tag{6}$$

$$\frac{\partial^2 p_{i,j}}{\partial x^2} = \frac{p_{i,j+1}-2p_{i,j}+p_{i,j-1}}{\Delta x^2}, \quad \text{for} \quad i=1,\ldots,(M-1) \text{ and } j=2,\ldots,(N-1), \tag{7}$$

where $p_{i,j}$ is the pressure in the inner node with (s_i, x_j) coordinates. After substituting of Eqs. (4) – (7) into Eq. (1), we obtain

$$a_{i,j}\,p_{i+1,j}+b_{i,j}\,p_{i-1,j}+c_{i,j}\,p_{i,j}+d_{i,j}\,p_{i,j+1}+e_{i,j}\,p_{i,j-1}=f_{i,j}, \tag{8}$$

where $a_{i,j}, b_{i,j}, c_{i,j}, d_{i,j}, e_{i,j}, f_{i,j}$ are coefficients of the linear combination. Eq. (8) has to be arranged for each inner node of the mesh. The resulting system of equations can be written in the matrix form

$$\mathbf{A}\mathbf{p} = \mathbf{f}, \tag{9}$$

where $\mathbf{p}$ is the vector of unknown nodal pressure distribution in the inner nodes, $\mathbf{f}$ is the vector with the terms on the right side of the Reynolds equation (1). Vector $\mathbf{f}$ also includes terms from Eq. (8) which respect the boundary conditions [1]. Coefficient matrix $\mathbf{A}$ is sparse, symmetric and positive definite.

The components of hydrodynamic forces can be evaluated by direct integration of pressure distribution as

$$F_{hd,y} = -\int_{-l/2}^{l/2}\int_{0}^{2\pi r} p\cos\left(\frac{s}{r}\right)\mathrm{d}s\,\mathrm{d}x, \qquad F_{hd,z} = -\int_{-l/2}^{l/2}\int_{0}^{2\pi r} p\sin\left(\frac{s}{r}\right)\mathrm{d}s\,\mathrm{d}x. \tag{10}$$

Because Eq. (9) yields the vector of nodal pressures, integrals from Eq. (10) can be expressed in the form of finite sums

$$F_{hd,y} = -\sum_{i=1}^{M}\sum_{j=1}^{N} p_{i,j}\Delta x\Delta s\cos\frac{s_i}{r}, \qquad F_{hd,z} = -\sum_{i=1}^{M}\sum_{j=1}^{N} p_{i,j}\Delta x\Delta s\sin\frac{s_i}{r}. \tag{11}$$

Hydrodynamic forces $F_{hd,y}$ and $F_{hd,z}$ are obviously non-linear. However, if the journal performs small motions around its equilibrium position, the hydrodynamic forces can be linearised and represented by the above-mentioned dynamic coefficients. The forces are then given by the following relation [2]

$$\begin{bmatrix} F_{hd,y} \\ F_{hd,z} \end{bmatrix} = -\begin{bmatrix} k_{yy} & k_{yz} \\ k_{zy} & k_{zz} \end{bmatrix}\begin{bmatrix} y \\ z \end{bmatrix} - \begin{bmatrix} b_{yy} & b_{yz} \\ b_{zy} & b_{zz} \end{bmatrix}\begin{bmatrix} \dot{y} \\ \dot{z} \end{bmatrix}. \tag{12}$$

Coefficients of stiffness k_{ij} and damping b_{ij} from Eq. (12) are generally derived from the Taylor series of the hydrodynamic force at the equilibrium position [2]. Appropriate partial derivatives can be rewritten in the form of finite differences

$$k_{ij} = -\frac{\Delta F_{hd,i}}{\delta_j}, \qquad b_{ij} = -\frac{\Delta F_{hd,i}}{\dot{\delta}_j}, \tag{13}$$

where subscripts i, j indicate the vertical and the horizontal directions y and z, respectively, δ_j is a small displacement from the equilibrium position, $\dot{\delta}_j$ is a velocity of the squeeze effect and $\Delta F_{hd,i}$ is the difference of the component of hydrodynamic force at the equilibrium position and under new conditions. The exact specification of how to evaluate the dynamic coefficients is presented in Fig. 2.

3 Numerical analysis of hydrodynamic forces

The finite difference method introduced in the previous section has certain limitations, which are apparent e.g. in [8, 9]. These limitations are introduced and described in this section. Firstly, parameters of the analysed model are summarised and then results are shown and discussed in detail.

3.1 Model and simulation parameters

Parameters of the analysed model are presented in Tab. 1. Note that two variables were independently changed during the course of the analysis — journal speed n was varied with step $\Delta n = 10$ rpm and the number of nodes in circumferential direction M was varied with step $\Delta M = 10$. Calculations presented in Fig. 2 are performed for all possible combinations of n and M.

Parameter p_a from Tab. 1 specifies hydrodynamic pressure at the edges of the bearing and parameter p_c is used in the model of cavitation which is implemented as follows: if hydrodynamic pressure p in any node of the mesh drops below the predefined value p_c, then $p = p_c$ is set in that particular node.

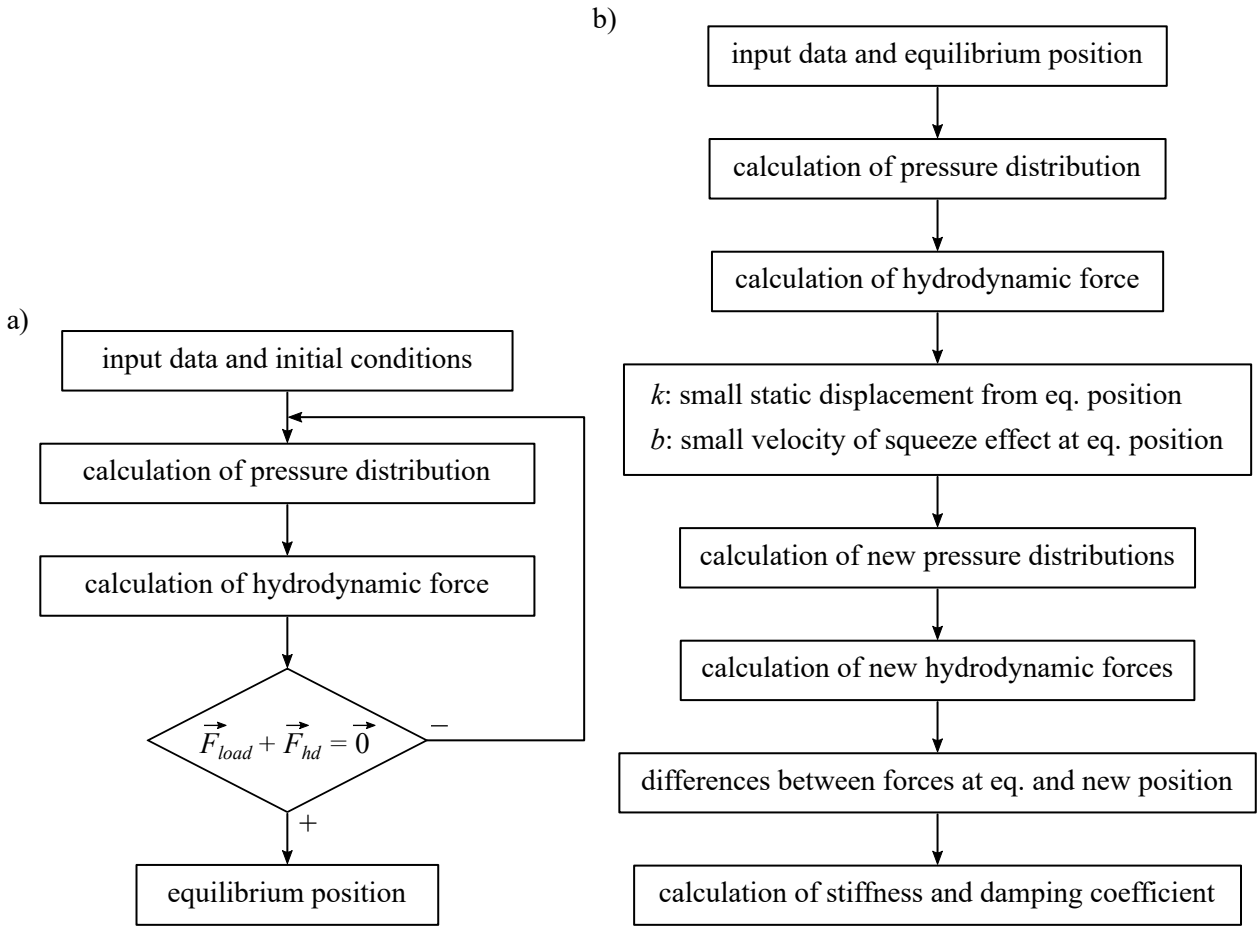

Fig. 2: a) A flow chart of the algorithm for the calculation of the equilibrium position and b) a flow chart of the algorithm for the calculation of stiffness and damping coefficients

bearing radius	r	(mm)	49.37
bearing length	l	(mm)	49.37
radial clearance	c_r	(mm)	0.9
journal speed	n	(rpm)	1000–5000
bearing load	F_{load}	(N)	98
oil viscosity	μ	(Pa·s)	0.07
ambient pressure	p_a	(bar)	0
saturation pressure	p_c	(bar)	0
number of nodes in axial direction	N	(-)	21
number of nodes in circumferential direction	M	(-)	30–170

Tab. 1: Parameters of the analysed model are partially based on [10]

3.2 Results

Let us introduce a new dimensionless quantity called relative eccentricity ε, which is defined as

$$\varepsilon = \frac{e}{c_r}. \tag{14}$$

The dependence of relative eccentricity of the equilibrium point on speed n and on the number of nodes in circumferential direction M is shown in Fig. 3a. Apparently, there are no visible differences between results obtained with models with low value of M and high value of M apart from the case $M = 30$. However, further investigation of ε reveals that ε is not a smooth function. In fact, not even the first derivative with respect to n is continuous as shown in Fig. 3b.

These small errors of the results are caused by a non-linear character of conditions for the equilibrium, see Fig. 2a, or by ill-conditioning of these conditions. The observed errors propagates through the algorithm and cause further errors of the numerically evaluated hydrodynamic forces. Although the discontinuities are negligible in the case of the components in the Cartesian coordinate system $F_{hd,y}$ and $F_{hd,z}$, they are rather prominent in the coordinate system with radial and tangential axes (Fig. 3c). Moreover, some parameters are strongly dependent on the size of the mesh — most notably maximum hydrodynamic pressure p_{max} and the position of p_{max} in the bearing (Fig. 3d).

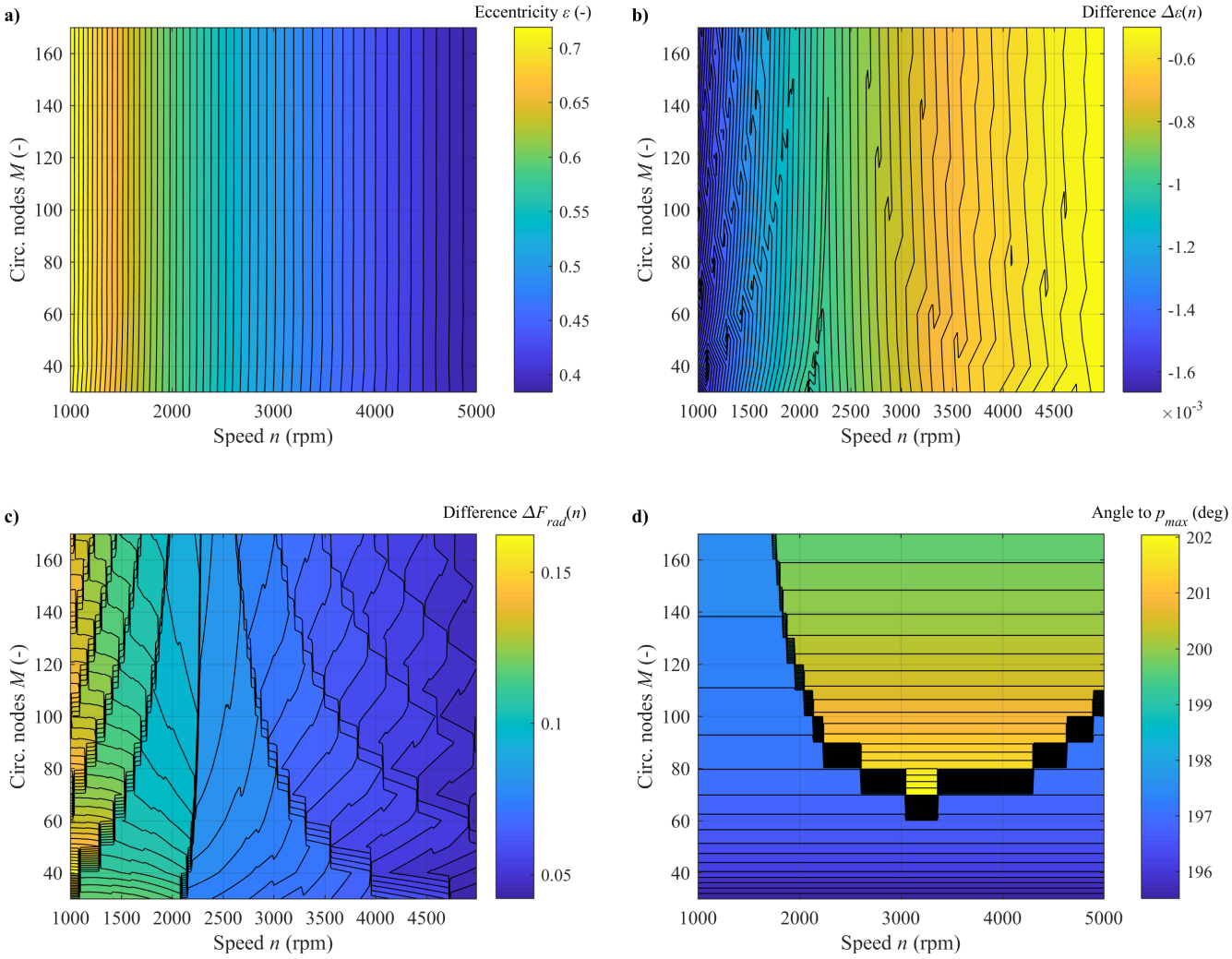

Fig. 3: Contour plots show a) relative eccentricity of equilibrium point ε, b) difference of relative eccentricity ε with respect to n, c) difference of the radial component of hydrodynamic force F_{rad} with respect to n, and d) angle to maximum pressure as the functions of speed n and of the number of nodes in circumferential direction M

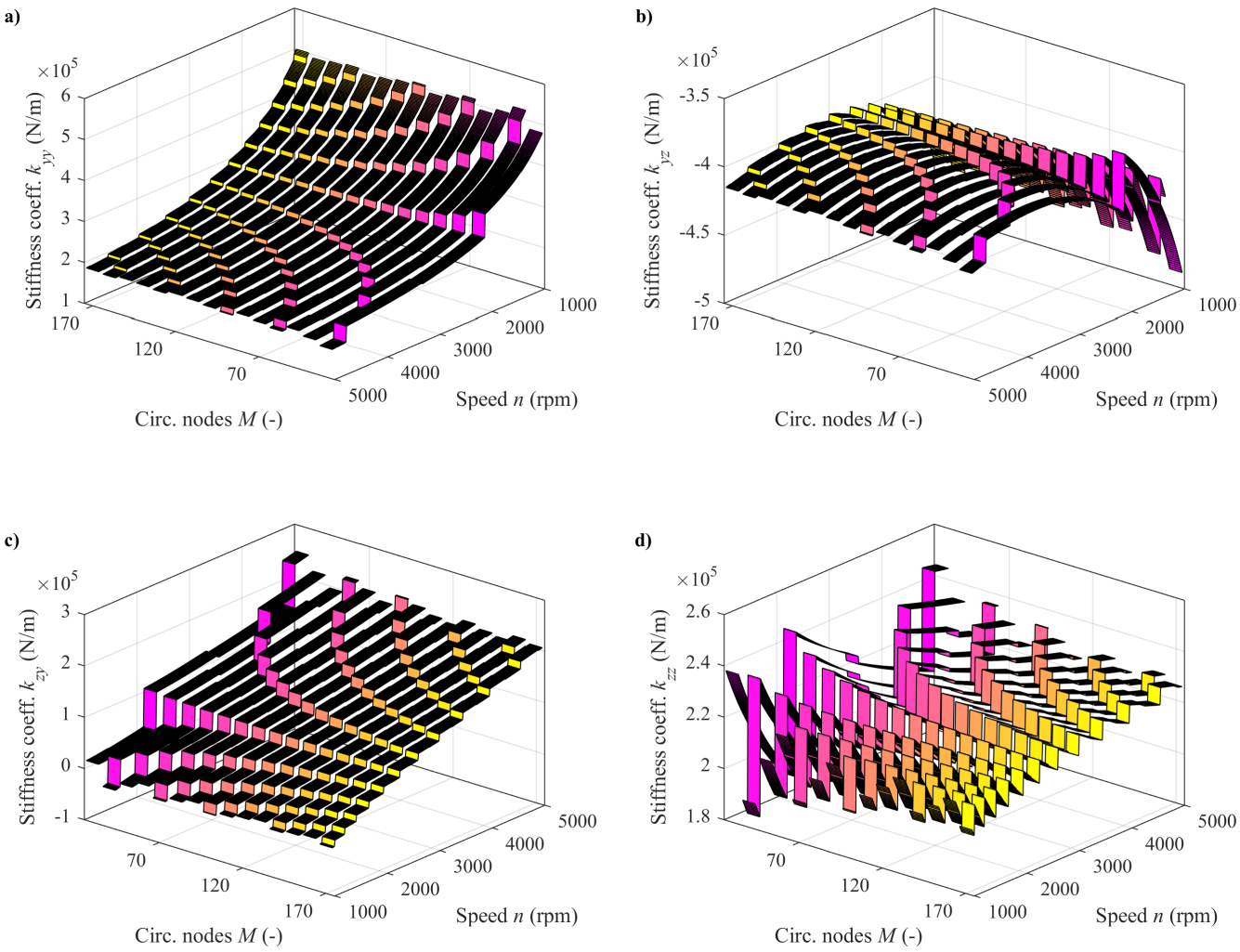

Fig. 4: Coefficients of stiffness plotted against speed n and the number of circumferential nodes M. Note that figures a) and b) have reversed n axis in comparison with figures c) and d)

The errors in the determination of ε and of the hydrodynamic forces are negligible if these parameters are evaluated directly. However, if the hydrodynamic forces are linearised, the non-smoothness of ε, $F_{hd,y}$ and $F_{hd,z}$ translates into jump discontinuities of a function which describes the dependence of the dynamic coefficients on speed n. These jump discontinuities of the stiffness coefficients are depicted in Fig. 4 and similar discontinuities can also be observed in the case of the damping coefficients. Interestingly, for lower values of M there is a lower number of jump discontinuities and bigger jumps and vice versa, for higher values of M there is a higher number of discontinuities and smaller jumps. Note that the discontinuities may not be apparent if the coefficients are evaluated in a low number of speeds.

4 Conclusions

This work has provided a basic overview of the evaluation of the hydrodynamic forces in journal bearings by means of the finite difference method. This method can also be used for the evaluation of the forces in hydrodynamic films between pistons and liners, in linear and radial aerodynamic bearings and in other lubricated contacts.

Furthermore, some limitations of the finite difference method are addressed and discussed — most notably the non-smoothness of the function which describes the dependence of the equilibrium point on the speed. The non-smoothness is caused by a non-linear character of conditions for the equilibrium, or by a ill-conditioning of these conditions.

The errors due to the non-smoothness cause errors in the hydrodynamic forces. These errors are negligible if the forces are evaluated directly but if the hydrodynamic forces are linearised, the non-smoothness translates into jump discontinuities of a function which describes the dependence of dynamic coefficients on speed n.

The obvious precaution against the jump discontinuities is to use as many points in the circumferential direction of the mesh as possible. Interestingly, this precaution helps only partially, because if more points are used, more discontinuities are present. An additional precaution is the usage of strict tolerances for the evaluation of the equilibria conditions.

Acknowledgements

This work was supported by the grant of the Czech Science Foundation No. 17-15915S entitled *Nonlinear dynamics of rotating systems considering fluid film instabilities with the emphasis on local effects*.

References

[1] G. W. Stachowiak and A. W. Batchelor, *Engineering Tribology*. St. Louis: Butterworth-Heinemann, 4th ed., 2013.

[2] E. Krämer, *Dynamics of Rotors and Foundations*. Berlin: Springer, 1993.

[3] L. R. Gero and C. M. McC. Ettles, "A three dimensional thermohydrodynamic finite element scheme for fluid film bearings," *Tribology Transactions*, vol. 31, no. 2, pp. 182–191, 1988.

[4] J. S. Larsen and I. F. Santos, "Efficient solution of the non-linear Reynolds equation for compressible fluid using the finite element method," *Journal of the Brazilian Society of Mechanical Sciences and Engineering*, vol. 37, no. 2, pp. 945–957, 2015.

[5] A. T. Prata, R. T. S. S. Ferriera, D. E. B. Mile and M. G. D. Bortoli, "Dynamically Loaded Journal Bearings: Finite Volume Method Analysis," in *Proceedings of the 1988 International Compressor Engineering Conference*, pp. 34–41, Purdue, Indiana, 1998.

[6] J. W. Lund and B. Sternlicht, "Rotor-Bearing Dynamics With Emphasis on Attenuation," *Journal of Basic Engineering*, vol. 84, no. 4., pp. 491–498, 1962.

[7] W. Weimin, Y. Lihua, W. Tiejun and Y. Lie, "Nonlinear dynamic coefficients prediction of journal bearings using partial derivative method," *Proceedings of the Institution of Mechanical Engineers, Part J: Journal of Engineering Tribology*, vol. 226, no. 4., pp. 328–339, 2012.

[8] O. Ebrat, Z. P. Zissimos, N. Vlahopoulos and K. Vaidyanathan, "Calculation of journal bearing dynamic characteristics including journal misalignment and bearing structural deformation," *Tribology Transactions*, vol. 47, no. 1, pp. 94–102, 2010.

[9] T. H. Machado and K. L. Cavalca, "Evaluation of dynamic coefficients for fluid journal bearings with different geometries," in *Proceedings of COBEM 2009*, pp. 1–11, November 15 – 20, Gramado, Brazil, 2009.

[10] Y. Bastani and M. de Queiroz, "A new analytic approximation for the hydrodynamic forces in finite-length journal bearings," *Journal of Tribology*, vol. 132, no. 1, pp. 014502–9, 2010.